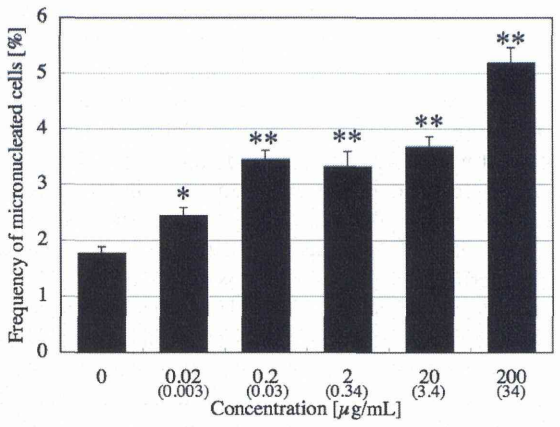

Fig. 1. Micronuclei formation in human A549 cells after 6 hours' treatment with magnetite nanoparticles. Mean ± S.D. values of at least 1,000 cells are shown. In the graph, 0 represents the solvent control (treatment with 0.005% (v/v) Tween 80). Concentrations in μg/cm² are given in parenthesis. There was a significant effect of concentration in one-way ANOVA ($p < 0.01$); $*p < 0.05$, $**p < 0.01$ (versus the solvent control) according to the Tukey-Kramer method.

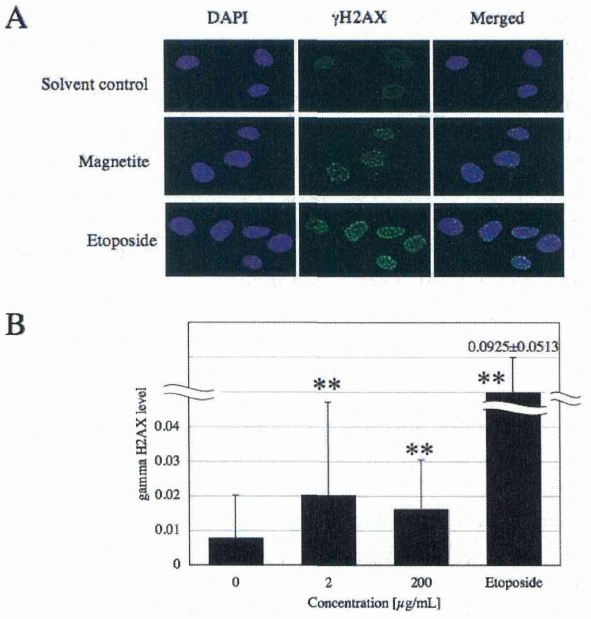

Fig. 2. γH2AX foci induced in A549 cells by 1 hour's treatment with magnetite nanoparticles. A, Magnified images of γH2AX foci in the cells treated with 0.005% (v/v) Tween 80 as a solvent control, 200 μg/ml magnetite nanoparticles, or 100 μg/ml etoposide as a positive control. B, Relative level of γH2AX. Mean ± S.D. values of at least 100 cells are shown. In the graph, 0 represents the solvent control (treatment with 0.005% (v/v) Tween 80). Etoposide (100 μg/ml) was used as a positive control. There was a significant effect of concentration of magnetite nanoparticles in one-way ANOVA ($p < 0.01$); $**p < 0.01$ (versus the solvent control) according to the Tukey-Kramer method.

for 24 hr) (Konczol *et al.*, 2011). We used Tween 80 as a surfactant to prepare the particle suspension. The difference in the dispersion procedure influences agglomeration of the particle, and might affect the toxicity in the low dose range.

In our experiment, the magnetite particles induced MN formation in CHO AA8 cells as well (Fig. 5A). The frequency rose to 5.0% at a magnetite concentration of 200 μg/ml (34 μg/cm²).

Formation of γ-H2AX foci

Since MN formation can be caused by DSB, the frequency of DSB in the cells treated with magnetite particles was evaluated by detecting phosphorylated H2AX (Fig. 2). The treatment of A549 cells with the nanoparticles for 1 hr induced H2AX phosphorylation (Fig. 2A). The relative levels of H2AX phosphorylation in the treated cells were two times higher than the control level (Fig. 2B), and the increase was significant ($p < 0.01$) at magnetite nanoparticle concentrations of 2 μg/ml or higher. In addition to DSB, various other forms of DNA damage can also induce the formation of γH2AX foci since DNA damage induces replication arrest, which causes DSB (Friedberg *et al.*, 2006). Therefore, the observed increase in the number of γH2AX foci indicates that the magnetite nanoparticles induced DSB in a direct or indirect manner in the A549 cells. Using the comet assay, Konczol *et al.* (2011) also detected increased DNA migration in A549 cells that had been treated with magnetite nanoparticles, which was indicative of treatment-induced DNA damage. Our findings are consistent with theirs.

Induction of SCE

DNA damage including DSB is known to induce SCE. Thus, we evaluated the clastogenic activity of magnetite nanoparticles using the SCE test. It is easier to observe chromatids in Chinese hamster cells than in human cells since Chinese hamster cells have fewer chromosomes than humans. As the magnetite particles induced MN formation in the CHO AA8 cells as well (Fig. 5A), we performed the SCE test using CHO AA8 cells (Fig. 3). An SCE frequency of approximately five times the control

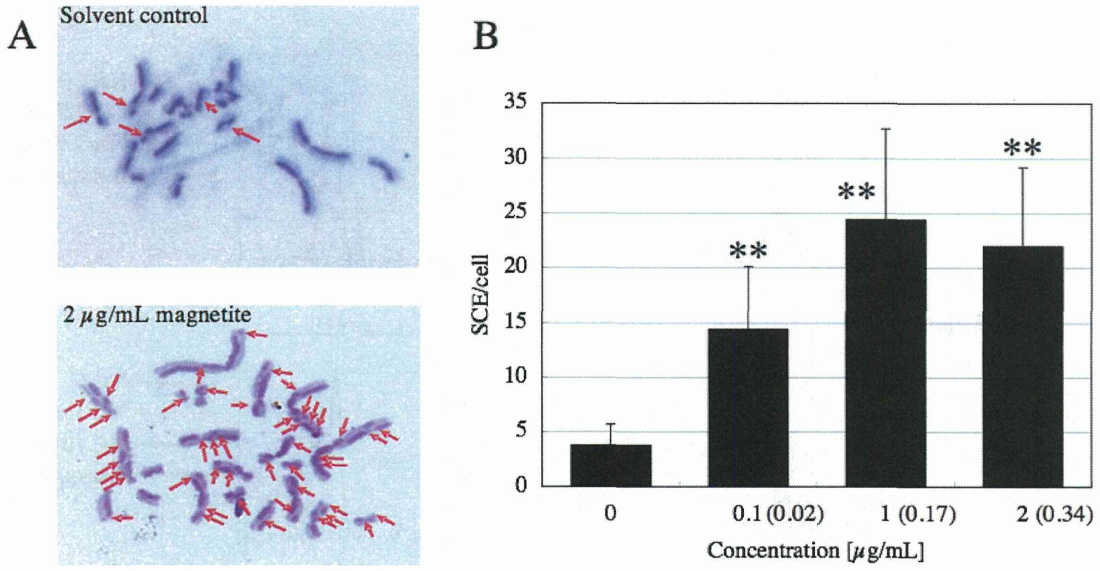

Fig. 3. SCE in CHO AA8 cells following 1 hour's treatment with magnetite nanoparticles. A, Typical images of SCE. The arrows indicate the locations of SCE. B, The number of SCE events per cell. Mean ± S.D. values of at least 50 cells are shown. In the graph, 0 represents the solvent control (treatment with 0.005% (v/v) Tween 80). Concentrations in μg/cm² are given in parenthesis. There was a significant effect of concentration in one-way ANOVA ($p < 0.01$); $^{**}p < 0.01$ (versus the solvent control) according to the Tukey-Kramer method.

level was observed in the cultures treated with 2 μg/ml (0.34 μg/cm²) of the magnetite particles. This increase was significant ($p < 0.01$) at concentrations of 0.1 μg/ml (0.017 μg/cm²) or higher. This is the first report to find that magnetite nanoparticles induce SCE in mammalian cells. The results of the MN and SCE tests indicate that magnetite nanoparticles have clastogenic potency in cultured mammalian cells.

Generation of reactive oxygen species

The generation of ROS in CHO cells that had been treated with magnetite particles was examined using FCM. After the cells had been treated with the particles for 1.5 hr, dose-dependent increases in the numbers of ROS signals were detected (Fig. 4A). Whereas only 9.8% of the cells displayed fluorescent intensity of greater than 10^4 arbitrary unit in the solvent control, treatment with magnetite particle concentrations of 2 μg/ml and 20 μg/ml resulted in 19.8% and 95.5% of the cells displaying fluorescent intensity of greater than 10^4 arbitrary unit, respectively. The number of ROS signals was decreased in the presence of anti-oxidants (Fig. 4B). The addition of NAC, ascorbic acid (vitamin C), or α-tocopherol (vitamin E) decreased the fluorescent intensity of the cells. Ascorbic acid and α-tocopherol reduced ROS to a greater degree than NAC. These results indicate that the magnetite particles induced ROS production in the CHO cells. Increase of ROS signals in A549 cells treated with magnetite particles and decrease of the signals in the presence of NAC were also observed (data not shown). Previous studies have also detected ROS generation in A549 cells treated with magnetite nanoparticles (Konczol *et al.*, 2011).

The mechanism of ROS production by magnetite is still unclear. Particles can damage mitochondria, therefore, interaction between magnetite and mitochondria could be responsible to the ROS generation (Konczol *et al.*, 2011). Membrane-bound NADPH oxidases could enhance production of ROS as well. Uptake of particles via phagocytosis can lead to an activation of the membrane-bound NADPH oxidase, which catalyzes the conversion of oxygen to superoxide radicals (Konczol *et al.*, 2011; Nabeshi *et al.*, 2011).

Note that although treatment with the particle concentrations of 20 μg/ml induced much higher ROS signals than that with 2 μg/ml, the genotoxic effects were similar

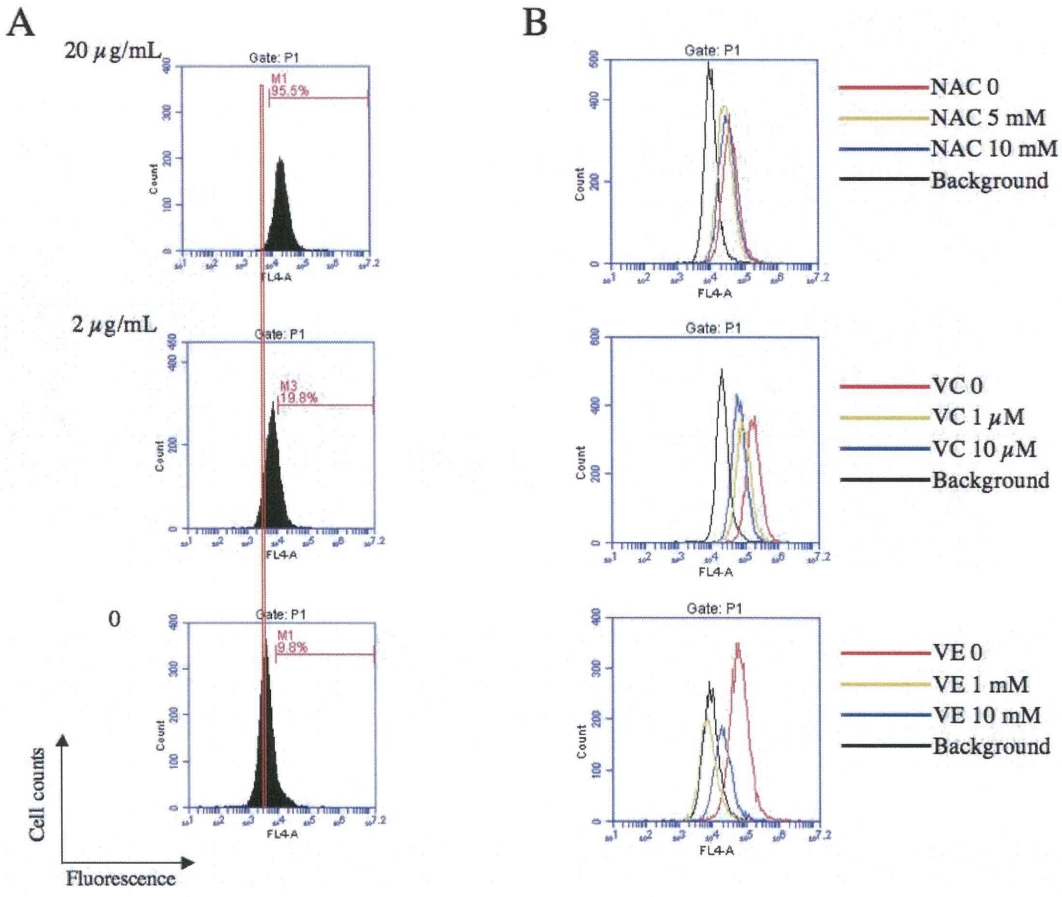

Fig. 4. Flow cytometric analysis of ROS production in CHO AA8 cells after treatment with magnetite nanoparticles. A, Distribution of ROS signals (fluorescence produced by CellROX Deep Red) in the cells treated with the indicated concentrations of magnetite for 1.5 hr. The vertical red line indicates the maximum distribution of fluorescent signals in the solvent control cells. The percentage of cells that displayed fluorescent intensity of greater than 10^4 arbitrary unit is shown in each graph. B, Distribution of ROS signals in the cells treated with 2 μg/ml magnetite nanoparticles in the presence of various anti-oxidants. NAC, VC, and VE represent *N*-acetylcysteine, ascorbic acid, and α-tocopherol, respectively. Background represents the distributions of cellular fluorescent intensity in the cells treated with anti-oxidants (10 mM NAC or VE, or 10 μM VC) in the absence of magnetite nanoparticles.

between these two doses (Figs. 4 and 5A). Cellar defense mechanism against oxidative stress might affect the genotoxicities.

Reduction of micronucleus formation by anti-oxidants

We investigated the relationship between ROS induction and the clastogenicity of the magnetite particles in mammalian cells. As described above, the magnetite treatment induced MN formation in CHO AA8 cells (Fig. 5A). In the presence of the anti-oxidant NAC, the frequency of micronucleated cells among the cells treated with magnetite nanoparticles was decreased in an NAC-dose dependent manner (Fig. 5B). Among the cells treated with 20 μg/ml (3.4 μg/cm^2) magnetite particles, treatment with 5 mM and 10 mM NAC resulted in micronucleated cell frequencies of 72% and 54% of those observed in the absence of NAC, respectively. Konczol *et al.* (2011) also reported decreased MN formation in the presence of NAC, therefore, our data are consistent with theirs. Another anti-oxi-

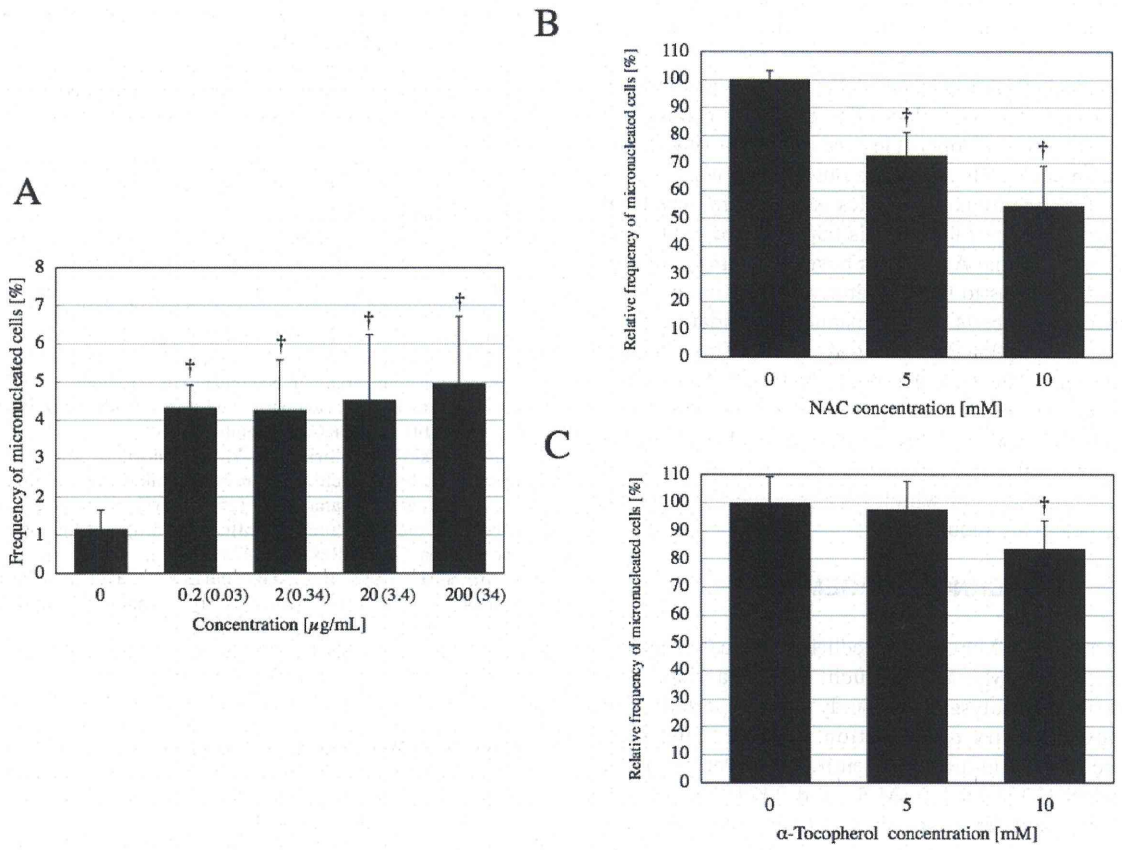

Fig. 5. Decrease in the micronuclei frequency of CHO AA8 cells induced by magnetite nanoparticle treatment in the presence of anti-oxidants. A, Frequency of micronucleated cells among the CHO AA8 cells after 6 hours' treatment with magnetite nanoparticles. Concentrations in μg/cm² are given in parenthesis. †$p < 0.05$ (versus the solvent control) according to the Student's t-test. B and C, Frequency of MN induction in the presence of NAC (B) or α-tocopherol (C). The frequency of micronucleated cells among the cells treated with 20 μg/ml magnetite nanoparticles in the absence of the anti-oxidants was regarded as 100%. Mean ± S.D. values of at least 1,000 cells are shown; †$p < 0.05$ (versus the absence of anti-oxidants) according to the Student's t-test.

dant, α-tocopherol, also reduced the frequency of MN, and it produced a significant reduction in the MN frequency at a concentration of 10 mM. However, the ability of the anti-oxidants to reduce the frequency of MN was not concordant with their effects on ROS. For example, in the MN test NAC reduced the MN frequency to a greater degree than α-tocopherol, whereas α-tocopherol eliminated ROS more efficiently than NAC (Fig. 4B and Figs. 5B, C). The reason for this is unclear; however, ROS might not be the sole cause of the genotoxicity/clastogenicity of magnetite nanoparticles.

In conclusion, we found that manufactured magnetite nanoparticles displayed genotoxicity in *in vitro* assay systems. Our data indicate that magnetite nanoparticles induce ROS production in mammalian cells, leading to the induction of DNA strand breaks directly or indirectly through oxidative DNA damage, followed by clastogenic events including MN formation and SCE. Our observations in A549 cells are consistent with the previous study (Konczol *et al.*, 2011). On the other hand, we observed ROS and MN inductions in CHO cells although Guichard *et al.* (2012) reported that the particles did not increase the ROS or MN formation in Syrian hamster embryo cells. This inconsistency indicates that difference

in cell types and species (genus) would influence the biological effect induced by magnetite nanoparticles. The concentrations of the particles tested in the present study are extremely high compared with the levels encountered by humans in the workplace. Therefore, we cannot conclude magnetite nanoparticles are imminent risk factors on human health. However, the observed *in vitro* genotoxicity of magnetite nanoparticles is a concern because of the large number of individuals that are exposed to such particles. Note that A549 cells have a mutation in keap1 gene, which leads to the constitutive activation of NRF2 that affords the cells with resistance to oxidative stress (Singh *et al.*, 2006; Homma *et al.*, 2009). This nature of the cells may affect the genotoxicity, therefore, genotoxicity assays using A549 cells might underestimate the risk of magnetite nanoparticles. Therefore, further studies on the genotoxicity mechanisms of magnetite particles and the concentrations at which they become hazardous to human health are required.

ACKNOWLEDGEMENTS

We thank Ms. M Fujii for excellent technical assistance. We also thank Ms. M Taniguchi for her assistance to the statistical analyses. This study was supported by the Japanese Ministry of Education, Science, Sports and Culture (Grants-in-aid for Scientific Research for Young Scientists (23710081 to M.K. and 23710084 to K.I.) and for Scientific Research (B) (24310047 to T.Y.)). This study was also supported by the Japanese Ministry of Health, Labor and Welfare (Grants-in-aid for Cancer Research (M.K. and Y.T.) and for Research on the Risk of Chemical Substances (Y.T.)), and a grant from the Japan Chemical Industry Association (JCIA) Long-range Research Initiative (LRI) (Y.T.).

REFERENCES

Ankamwar, B., Lai, T.C., Huang, J.H., Liu, R.S., Hsiao, M., Chen, C.H. and Hwu, Y.K. (2010): Biocompatibility of Fe_3O_4 nanoparticles evaluated by *in vitro* cytotoxicity assays using normal, glia and breast cancer cells. Nanotechnology, **21**, 75102.

Bosi, S., Da Ros, T., Spalluto, G. and Prato, M. (2003): Fullerene derivatives: an attractive tool for biological applications. Eur. J. Med. Chem., **38**, 913-923.

Donaldson, K., Tran, L., Jimenez, L.A., Duffin, R., Newby, D. E., Mills, N., MacNee, W. and Stone, V. (2005): Combustion-derived nanoparticles: a review of their toxicology following inhalation exposure. Part. Fibre Toxicol., **2**, 10.

Elmore, A.R. (2003): Cosmetic Ingredient Review Expert Panel: Final report on the safety assessment of aluminum silicate, calcium silicate, magnesium aluminum silicate, magnesium silicate, magnesium trisilicate, sodium magnesium silicate, zirconium silicate, attapulgite, bentonite, Fuller's earth, hectorite, kaolin, lithium magnesium silicate, lithium magnesium sodium silicate, montmorillonite, pyrophyllite, and zeolite. Int. J. Toxicol., **22 Suppl. 1**, 37-102.

Figuerola, A., Di, C.R., Manna, L. and Pellegrino, T. (2010): From iron oxide nanoparticles towards advanced iron-based inorganic materials designed for biomedical applications. Pharmacol. Res., **62**, 126-143.

Friedberg, E.C., Walker, G.C., Siede, W., Wood, R.D., Schultz, R.A. and Ellenberger, T. (2006): DNA repair and Mutagenesis, ASM press, Washington, D.C., USA.

Guichard, Y., Schmit, J., Darne, C., Gaté, L., Goutet, M., Rousset, D., Rastoix, O., Wrobel, R., Witschger, O., Martin, A., Fierro, V. and Binet, S. (2012): Cytotoxicity and genotoxicity of nanosized and microsized titanium dioxide and iron oxide particles in Syrian hamster embryo cells. Ann. Occup. Hyg., **56**, 631-644.

Hoet, P., Bruske-Hohlfeld, I. and Salata, O. (2006): Possible health impact of nanomaterials. In Nanomaterials - Toxicity, health and environmental issues (Kumar C., ed.), pp.53-80, WILEY-VGH Verlag GmbH & Co. KGaA, Weinheim.

Homma, S., Ishii, Y., Morishima, Y., Yamadori, T., Matsuno, Y., Haraguchi, N., Kikuchi, N., Satoh, H., Sakamoto, T., Hizawa, N., Itoh, K. and Yamamoto, M. (2009): Nrf2 enhances cell proliferation and resistance to anticancer drugs in human lung cancer. Clin. Cancer Res., **15**, 3423-3432.

Hussain, S.M., Hess, K.L., Gearhart, J.M., Geiss, K.T. and Schlager, J.J. (2005): *In vitro* toxicity of nanoparticles in BRL 3A rat liver cells. Toxicol. In Vitro, **19**, 975-983.

IARC (1996): Carbon Black and Some Nitro Compounds. In IARC Monogr. Eval. Carcinog. Risks Hum., **65**, 149-262.

Kato, T., Totsuka, Y., Ishino, K., Matsumoto, Y., Tada, Y., Nakae, D., Goto, S., Masuda, S., Ogo, S., Kawanishi, M., Yagi, T., Matsuda, T., Watanabe, M. and Wakabayashi, K. (2012): Genotoxicity of multi-walled carbon nanotubes in both *in vitro* and *in vivo* assay systems. Nanotoxicology. (in press). doi: 10.3109/17435390.2012.674571.

Konczol, M., Ebeling, S., Goldenberg, E., Treude, F., Gminski, R., Giere, R., Grobety, B., Rothen-Rutishauser, B., Merfort, I. and Mersch-Sundermann, V. (2011): Cytotoxicity and genotoxicity of size-fractionated iron oxide (magnetite) in A549 human lung epithelial cells: role of ROS, JNK, and NF-κB. Chem. Res. Toxicol., **24**, 1460-1475.

Lewinski, N., Colvin, V. and Drezek, R. (2008): Cytotoxicity of nanoparticles. Small, **4**, 26-49.

Mazzola, L. (2003): Commercializing nanotechnology. Nat. Biotechnol., **21**, 1137-1143.

Nabeshi, H., Yoshikawa, T., Matsuyama, K., Nakazato, Y., Tochigi, S., Kondoh, S., Hirai, T., Akase, T., Nagano, K., Abe, Y., Yoshioka,Y., Kamada, H., Itoh, N., Tsunoda, S. and Tsutsumi, Y. (2011): Amorphous nanosilica induce endocytosis-dependent ROS generation and DNA damage in human keratinocytes. Part. Fibre Toxicol., **8**, 1.

Oberdorster, G., Oberdorster, E. and Oberdorster, J. (2005): Nanotoxicology: An emerging discipline evolving from studies of ultrafine particles. Environ. Health Perspect., **113**, 823-839.

Park, E.J., Kim, H., Kim, Y., Yi, J., Choi, K. and Park, K. (2010): Inflammatory responses may be induced by a single intratracheal instillation of iron nanoparticles in mice. Toxicology, **275**, 65-71.

Paull, R., Wolfe, J., Hebert, P. and Sinkula, M. (2003): Investing in nanotechnology. Nat. Biotechnol., **21**, 1144-1147.

Peters, A., Wichmann, H.E., Tuch, T., Heinrich, J. and Heyder, J. (1997): Respiratory effects are associated with the number of

ultrafine particles. Am. J. Respir. Crit. Care Med., **155**, 1376-1383.

Pickard, M.R. and Chari, D.M. (2010): Robust uptake of magnetic nanoparticles (MNPs) by central nervous system (CNS) microglia: Implications for particle uptake in mixed neural cell populations. Int. J. Mol. Sci., **11**, 967-981.

Schulz, H., Harder, V., Ibald-Mulli, A., Khandoga, A., Koenig, W., Krombach, F., Radykewicz, R., Stampfl, A., Thorand, B. and Peters, A. (2005): Cardiovascular effects of fine and ultrafine particles. J. Aerosol. Med., **18**, 1-22.

Shimohara, C. Sawai, T. and Yagi, T. (2008): Polyaromatic hydrocarbons cause histone H2AX phosphorylation in the S-phase of the Cell Cycle. Genes Env., **30**, 92-99.

Singh, A., Misra, V., Thimmulappa, R.K., Lee, H., Ames, S., Hoque, M.O., Herman, J.G., Baylin, S.B., Sidransky, D., Gabrielson, E., Brock, M.V. and Biswal, S. (2006): Dysfunctional KEAP1-NRF2 interaction in non-small-cell lung cancer. PLoS Med., **3**, 1865-1876.

Totsuka, Y., Higuchi, T., Imai, T., Nishikawa, A., Nohmi, T., Kato, T., Masuda, S., Kinae, N., Hiyoshi, K., Ogo, S., Kawanishi, M., Yagi, T., Ichinose, T., Fukumori, N., Watanabe, M., Sugimura, T. and Wakabayashi, K. (2009): Genotoxicity of nano/microparticles in *in vitro* micronuclei, *in vivo* comet and mutation assay systems. Part. Fibre Toxicol., **6**, 23.

Upadhyay, D., Panduri, V., Ghio, A. and Kamp, D.W. (2003): Particulate matter induces alveolar epithelial cell DNA damage and apoptosis: Role of free radicals and the mitochondria. Am. J. Respir. Cell Mol. Biol., **29**, 180-187.

J Toxicol Pathol 2013; 26: 393–403

Original Article

Long-term Pulmonary Responses to Quadweekly Intermittent Intratracheal Spray Instillations of Magnetite (Fe_3O_4) Nanoparticles for 52 Weeks in Fischer 344 Rats

Yukie Tada[1*], Norio Yano[1], Hiroshi Takahashi[1], Katsuhiro Yuzawa[1], Hiroshi Ando[1], Yoshikazu Kubo[1], Akemichi Nagasawa[1], Akiko Inomata[1], Akio Ogata[1], and Dai Nakae[1,2*]

[1] Department of Pharmaceutical and Environmental Sciences, Tokyo Metropolitan Institute of Public Health, 3-24-1 Hyakunin-cho, Shinjuku, Tokyo 169-0073, Japan
[2] Tokyo University of Agriculture, 1-1-1 Sakura-ga-Oka, Setagaya, Tokyo 156-8502, Japan

Abstract: Information about potential risks of iron nanomaterials is still limited, while a wide variety of applications are expected. We recently reported acute phase responses of male and female Fischer 344 rats after a single intratracheal spray instillation of Fe_3O_4 nanoparticles (magnetite), clearly showing dose-dependent pulmonary inflammatory changes (Tada *et al.*, J Toxicol Pathol 25, 233–239, 2012). The present study assessed long-term responses of male and female Fischer 344 rats to multiple administrations of magnetite. Ten-week-old male and female Fischer 344 rats (n=20/group) were exposed to a total of 13 quadweekly intermittent intratracheal spray instillations of magnetite during the experimental period of 52 weeks, at doses of 0, 0.2 (low), 1.0 (medium) and 5.0 (high-dose) mg/kg body weight per administration. Absolute and relative lung weights of the high-dose group were significantly higher than those of the control group. Macroscopically, slight enlargement and scattered black patches were recognized in the lungs and the lung-associated lymph nodes of the high-dose group. Histopathologically, infiltration of macrophages phagocytosing magnetite (all dose groups) and of chronic inflammatory cells (medium- and high-dose males and high-dose females), alveolar bronchiolization and granuloma (high-dose group) were observed. In addition, alveolar hyperplasias were observed in some rats of the high-dose group, and cytoplasmic overexpression of β-catenin protein was immunohistochemically found in such lesions. The present results clearly show that instilled magnetite causes chronic inflammatory responses in the lung. These responses occur in a dose-dependent manner without apparent differences among sexes (DOI: 10.1293/tox.2013-0036; J Toxicol Pathol 2013; 26: 393–403)

Key words: magnetite, Fe_3O_4, nanoparticles, lung, intratracheal spray instillation, Fischer 344 rat

Introduction

Engineered nanoparticles can have unique photonic and catalytic properties that display great differences from those of over-nanoscaled materials with the same composition. The superb biological and environmental reactivities of nanoparticles have led to their wide and considerable use in disease treatment, pollutant degradation and so forth[1]. Iron nanomaterials are a typical example and are attracting attentions due to their superparamagnetic characteristics and high catalytic abilities. It is expected that iron nanomaterials can be applied to a wide variety of fields such as environmental catalysis, magnetic storage, biomedical imaging[1], magnetic target drug delivery[2] and hyperthermia[3,4].

While information about potential risks of magnetite is still limited, there are several reports describing some toxicologic findings for magnetite[5–13]. In *in vitro* studies using L-929 murine fibroblastic cells, iron oxide nanoparticles affected cell viability and DNA stability[5], while in human alveolar epithelial-like type-II cells (A549), a micronucleus test and comet assay showed genotoxicity of magnetite[6]. *In vivo* studies with Fe_3O_4 particles caused inflammatory changes in rats exposed to pigment-sized particles through inhalation[7,8]. Magnetic nanoparticles of Fe_3O_4 affected the immune system of ICR mice, enhancing production of cytokines like interleukin (IL)-2, interferon-γ and IL-10 (but not IL-4) in the peripheral blood[9]. A high amount of magnetite, 15 mg × 15 intratracheal instillations, unexpectedly resulted in development of lung tumors in female Wistar rats[10], while chronic exposure to iron oxide did not increase the incidence of pulmonary tumors of rats[7,11]. Recently, we reported acute phase responses of male and female Fischer 344 rats 14 days after a single intratracheal spray instillation of magnetite (Fe_3O_4) nanoparticles, clearly showing that magnetite

Received: 3 July 2013, Accepted: 13 August 2013
*Corresponding authors: Y Tada (e-mail: Yukie_Tada@member.metro.tokyo.jp), D Nakae (e-mail: agalennde.dai@nifty.com)

caused foreign body inflammatory and granulating lesions in the lung in a dose-dependent manner[12]. Our histopathological findings showed that magnetite-laden macrophages were seen not only in the alveolar space but also in the alveolar septa or interstitial space, even in the low-dose group given 5.0 mg/kg body weight, indicating the possibility of severe injury resulting from intratracheal administration of magnetite[12].

Iron is a transition metal that is considered to play a pivotal role in modulating oxidative stress and other biological responses[13,14], which are speculated to be the critical mechanisms in eliciting the adverse effects of iron particulate matter exposure. The Organization for Economic Cooperation and Development (OECD) has generated a list of 14 commercially important nanoparticulate materials, in order to explore the possible health effects and regulate occupational and nonoccupational exposure scenarios, and iron oxide is included in the list[15]. In this context, it is apparently important to accumulate data regarding the toxicity/safety of magnetite, especially for its chronic influence on the living organisms. The present study was thus conducted to assess pulmonary responses to long-term intermittent intratracheal spray instillations of Fe_3O_4 nanoparticles (magnetite) in male and female Fischer 344 rats.

Materials and Methods

Ethical considerations

The current study was performed principally in conformity with the Guidelines for the Toxicity Testing of Pharmaceuticals released by the Ministry of Health, Labour and Welfare of Japan (http://www.pmda.go.jp/ich/s/s4_93_8_10.pdf; http://www.pmda.go.jp/ich/s/s4a_99_4_5.pdf). The experimental protocol was approved by the Experiments Regulation Committee and Animal Experiment Committee of the Tokyo Metropolitan Institute of Public Health, prior to its execution. All the animals were handled in accordance with the Japanese Government Animal Protection and Management Law, Japanese Government Notification on Feeding and Safekeeping of Animals and the Guidelines for Animal Experimentation issued by the Japanese Association for Laboratory Animal Science[16].

Animals

A total of 168 male and female specific pathogen-free Fischer 344 (F344/DuCrlCrlj) rats were purchased at 8 weeks of age from Charles River Laboratories Japan, Inc. (Kanagawa, Japan). The rats were housed individually in stainless steel cages and were kept under controlled conditions of temperature (22–24°C), relative humidity (50–60%) and ventilation (more than 10 times/hour) with a 12-hr light/dark cycle. They were allowed free access to pelleted chow CE-2 (CLEA Japan, Inc., Tokyo, Japan) and drinking water throughout both the acclimation and experimental periods. After confirming normal health status at the end of the 2-week acclimation period, 80 rats of each sex were selected for use and randomly allocated to 4 groups of 20 rats. The rats were observed twice daily, and clinical signs and mortality were recorded. Body weight and food intakes were monitored weekly during the first 13 weeks, and were monitored every four weeks thereafter.

Test chemical and animal treatments

The magnetite slurry (Fe_3O_4 nanoparticle suspension; lot numbers, 90828 and 100316) was generously supplied by Toda Kogyo Corp. (Hiroshima, Japan). A representative transmission electron microscopic view of magnetite particles is shown in Fig. 1, and the primary particle size of the prepared sample was estimated to be 5–15 nm in diameter. The specific surface areas were determined to be 116.0 and 122.0 m^2/g for lot numbers 90828 and 100316, respectively, by the BET method. The purity of the test chemical was determined by an energy dispersive X-ray spectrometer, and only iron and oxygen were detected. Magnetite particles are poorly soluble in water. According to our previous report[12], magnetite slurry was diluted in sterile ultrapure water (vehicle: Milli-Q water, 18.2 MΩ) and adjusted to pH 7.4 with 0.1 M hydrochloric acid.

The intratracheal instillation technique was performed according to the recommendations of Driscoll *et al.*[17]. Before intratracheal spray instillation, the rats were anesthetized with diethyl ether and placed in a supine position on an angled board with their necks extended. Magnetite suspension was placed in an ultrasonication bath (Sonorex RK31, Bandelin Electronic, Berlin, Germany) set at a high frequency (35 kHz) and then inserted via the mouth into the bifurcation of trachea by a sterile stainless steel tube (IA-1B MicroSprayer, Penn-Century, Inc., Wyndmoor, PA, USA) at the concentrations of 0 (control: vehicle, 1.0 mL/kg body weight), 0.2 (low), 1.0 (medium) and 5.0 (high) mg/kg body weight, and this was followed by insufflation of 0.2 mL of air. The doses were decided based on the finding of

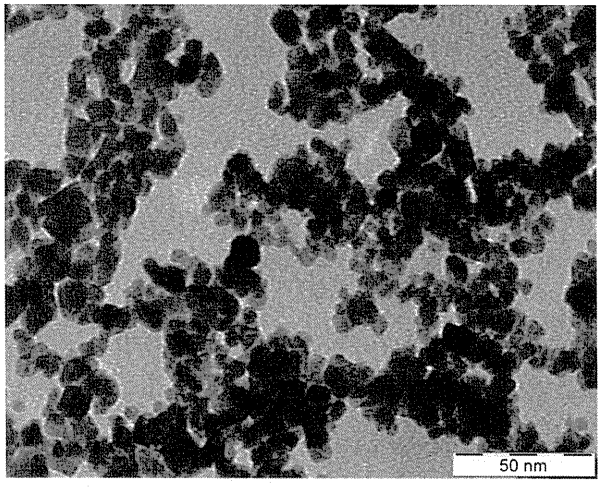

Fig. 1. Representative transmission electron microscopic view of magnetite nanoparticles. The estimated primary particle size is about 5–15 nm in diameter.

our acute single-dose toxicity study[12] showing that 15 mg/kg body weight of magnetite cannot be well dispersed in the lung and thus aggregated and filled in the alveoli. The rats were given a total of 13 quadweekly intermittent exposures during the experimental period of 52 weeks.

Animal sacrifice and assessments

Four weeks after the last instillation, all rats were deprived of food (but not water) overnight, and fresh urine samples were obtained for urinalysis of urobilinogen, occult blood, bilirubin, ketone, glucose, protein and pH using test papers (N-Multistix, Siemens Healthcare Diagnostics Inc., Tokyo, Japan). The rats were then lightly anesthetized by diethyl ether and sacrificed by exsanguination after collecting blood samples via the abdominal aorta. The blood for hematology was collected into tubes treated with dipotassium ethylenediaminetetraacetate. The hematological examination was carried out using an automatic analyzer (Sysmex KX-21NV, Sysmex Corporation, Hyogo, Japan) to determine the red blood cell count (RBC), hemoglobin concentration (HGB), hematocrit level (HCT), mean corpuscular volume (MCV), mean corpuscular hemoglobin (MCH), mean corpuscular hemoglobin concentration (MCHC), white blood cell count (WBC) and platelet count (PLT). A serum biochemistry analysis was performed with an automatic analyzer (TBA-120FR, Toshiba Medical Systems Corporation, Tokyo, Japan) to determine the levels of total protein (TP), albumin (ALB), albumin/globulin ratio (A/G), glucose (GLU), total cholesterol (T-CHO), triglyceride (TG), total bilirubin (T-BIL), aspartate aminotransferase (AST), alanine aminotransferase (ALT), alkaline phosphatase (ALP), blood urea nitrogen (BUN), creatinine (CRE), uric acid (UA), sodium (Na), potassium (K), chlorine (Cl) and calcium (Ca).

Upon sacrifice, the rats were macroscopically examined and subjected to a full autopsy. The brain, thyroids (with parathyroids), adrenal glands, lungs (including bronchi, fixed by inflation with fixative), heart, spleen, liver, kidneys, testes, ovaries and uterus were weighed and fixed in 10% neutrally buffered formalin. As well as these organs, the pituitary gland, sciatic nerve, spinal cords (cervical, mid-thoracic and lumbar), eyes, harderian glands, Zymbal's glands, thoracic aorta, nasal cavity, trachea, thymus, salivary glands, tongue, esophagus, stomach, duodenum, jejunum, ileum, caecum, rectum, pancreas, urinary bladder, epididymides, seminal vesicles, prostate, preputial glands, oviducts, vagina, skin with mammary glands, skeletal muscle, lymph nodes (submandibular and mesenteric), bones (femur and sternum) with bone marrow and all gross lesions of each animal were fixed. Paraffin-embedded sections were routinely prepared and histopathologically examined after being stained with hematoxylin and eosin, Azan-Mallory and Berlin blue procedures.

Immunohistochemistry was performed on 4-μm sections of the formalin-fixed paraffin embedded tissues, using a monoclonal mouse antibody to β-catenin (610153, BD Biosciences, San Jose, CA, USA). Heat-induced antigen retrieval with 10 mM citrate buffer, pH 6.0, was followed by incubation with the primary antibody (diluted to 1:100) at room temperature for 30 minutes. Detection of primary antibody binding was carried out with an EnVision antimouse/horseradish peroxidase-labeled polymer detection system (Dako North America Inc., Carpinteria, CA, USA) followed by visualization with 3,3'-diaminobenzidine (DAB) (Dako) and counterstaining with Mayer's hematoxylin. Negative control slides were subjected to the same staining protocol modified by the substitution of mouse normal IgG for the primary antibody.

Statistical analysis

For numerical data such as body and organ weights and hematological and serological outcomes, equality was assessed by Bartlett's test. Homogeneity of variance was then analyzed by one-way analysis of variance, and finally differences between the values of the control group and those of each treated group were evaluated by Dunnett's test. If the Bartlett's test was significant, the data were subjected to the Kruskal-Wallis test and Dunnett's-type rank sum test. For contingent data such as incidences of histopathological lesions, differences between the values of the control group and those of each treated group were evaluated by Fisher's exact probability test[18]. Statistical processing was conducted using the StatLight software (Yukms Co., Ltd., Tokyo, Japan). Intergroup differences were considered statistically significant, when P values less than 0.05 were obtained.

Results

General findings

Rats given magnetite (especially at the high dose) became less active than controls after instillation but recovered relatively soon. During the study, however, 3 low-dose males, 3 control females and 1, 2 and 4 low-, medium- and high-dose females, respectively, died due to deep anesthesia following magnetite administration. In addition, accidental deaths due to suffocation with the diet occurred in 3 medium-dose males, 3 control females and 2, 1 and 4 low-, medium- and high-dose females, respectively. As a result, the final effective numbers of rats were 20, 17, 17 and 20 for males and 14, 17, 17 and 12 for females in the control group and low-, medium- and high-dose groups, respectively. There were no significant differences in average body weights among groups throughout the experimental period for either sex (Fig. 2).

Urinalysis, hematology and serum biochemistry

In the urinalysis, no significant or treatment-related changes were observed in any analyzed parameters.

In the hematology, the MCHC values of the female control and low-, medium- and high-dose groups were 34.1 ± 0.8, 34.3 ± 0.6, 34.0 ± 0.6 and 33.4 ± 0.3 g/dL, respectively. Although the female high-dose value was significantly lower than the female control value, the change must lack a biological meaning or relation to the magnetite exposure,

because the slight decrease was not accompanied by any other hematological, serological or pathological relatedness. The WBC values of the male control and low-, medium- and high-dose groups were 32.8 ± 7.3, 30.0 ± 7.0, 30.0 ± 6.7 and 37.1 ± 10.7 $\times 10^2/\mu L$, respectively. The WBC values of the female control and low-, medium- and high-dose groups were 21.7 ± 6.1, 23.1 ± 6.6, 18.1 ± 3.5 and 21.8 ± 5.4 × $10^2/\mu L$, respectively. There were no significant differences in WBC data between the control and treated groups. No significant or treatment-related changes were observed in any other analyzed parameters.

In the serum biochemistry, the GLU values of the male control and low-, medium- and high-dose groups were 155.1 ± 16.6, 142.8 ± 15.5, 144.9 ± 15.5 and 139.1 ± 13.2 mg/dL, respectively, and the male low- and high-dose values were significantly lower than the male control value. The Na values of the male control and low-, medium- and high-dose groups were 140.8 ± 1.1, 141.3 ± 1.9, 141.7 ± 1.7 and 143.0 ± 1.6 mmol/L, respectively, and the male high-dose value was significantly higher than the male control value. The Na values of the female control and low-, medium- and high-dose groups were 141.4 ± 1.8, 142.6 ± 2.0, 144.7 ± 1.7 and 143.8 ± 1.3 mmol/L, respectively, and the female medium- and high-dose values were significantly higher than the female control group value. The Cl values of the male control and low-, medium- and high-dose groups were 104.6 ± 1.3, 105.8 ± 0.6, 105.4 ± 0.8 and 106.8 ± 1.0 mmol/L, respectively, and the male low- and high-dose values were significantly higher than the male control value. The Cl values of the female control and low-, medium- and high-dose groups were 105.8 ± 1.7, 106.2 ± 2.1, 108.2 ± 2.8 and 107.7 ± 1.6 mmol/L, respectively, and the female medium-dose value was significantly higher than the female control value. The Ca values of the female control and low-, medium- and high-dose groups were 10.2 ± 0.3, 10.5 ± 0.3, 10.4 ± 0.3 and 10.4 ± 0.3 mg/dL, respectively, and the female low- and medium- dose values were significantly higher than the female control value. These slight changes must lack a biological meaning or relation to the magnetite exposure, because they were not accompanied any other hematological, serological or pathological relatedness, and frequently did not show first-order dose-dependency. No significant or treatment-related changes were observed in any other analyzed parameters.

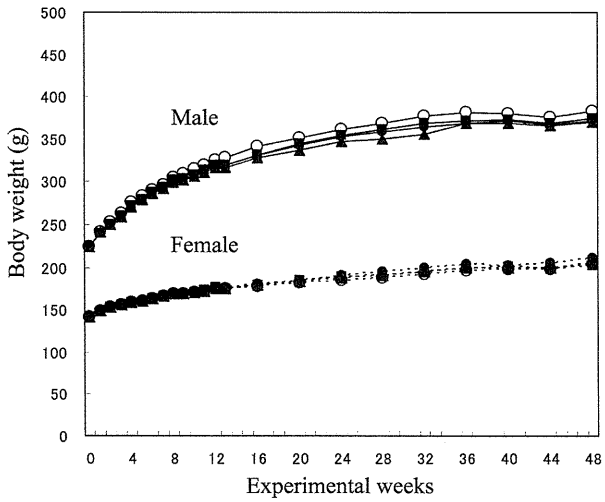

Fig. 2. Changes in mean body weights determined quadweekly for 52 weeks. The doses of magnetite were 0 (control) ○, 0.2 ●, 1.0 ▲ or 5.0 ■ mg/kg body weight per administration.

Pathology

While initial or final body weights were not different among groups, both absolute and relative lung weights of the high-dose group were significantly higher than the control value in both sexes (Table 1). The absolute weights of the thyroid glands of the male control and low-, medium- and high-dose groups were 21.0 ± 3.5, 17.7 ± 2.5, 21.4

Table 1. Initial and Final Body Weights and Lung Weights

Item	Dose of magnetite (mg/kg body weight)			
	0 (control)	0.2	1.0	5.0
Male				
Initial number of rats	20	20	20	20
Initial body weight (g)	224.1 ± 8.2[a]	223.5 ± 8.8	224.1 ± 7.9	223.4 ± 7.0
Final effective number of rats	20	17	17	20
Final body weight (g)	383.3 ± 20.3	372.1 ±20.1	370.0 ± 29.4	374.9 ± 23.0
Absolute lung weight (mg)	1017.4 ± 95.0	963.6 ± 57.8	1015.3 ± 60.7	1380.0 ± 82.2*
Relative lung weight (mg/100 g body weight)	278.7 ± 25.3	274.0 ± 17.5	289.8 ± 27.4	387.4 ± 24.1*
Female				
Number of rats	20	20	20	20
Initial body weight (g)	141.8 ± 4.9	141.4 ± 6.5	142.0 ± 5.5	142.2 ± 5.6
Final effective number of rats	14	17	17	12
Final body weight (g)	203.2 ± 17.8	210.9 ± 19.4	205.2 ± 19.2	202.6 ± 22.1
Absolute lung weight (mg)	729.3 ± 50.7	732.3 ± 63.5	722.3 ± 50.7	1086.2 ± 102.8*
Relative lung weight (mg/100 g body weight)	385.1 ± 45.1	372.5 ± 36.7	378.3 ± 40.5	559.0 ± 51.9*

[a] Values are means ± standard deviations, except those for animal numbers. * Significantly different from the corresponding control values ($P<0.05$, Dunnett's test).